6-1-2016

TNF and CD28 Signaling Play Unique but Complementary Roles in the Systemic Recruitment of Innate Immune Cells after Staphylococcus aureus Enterotoxin A Inhalation

Julia Svedova
University of Connecticut School of Medicine and Dentistry

Naomi Tsurutani
University of Connecticut School of Medicine and Dentistry

Wenhai Liu
University of Connecticut School of Medicine and Dentistry

Kamal M. Khanna
University of Connecticut School of Medicine and Dentistry

Anthony T. Vella
University of Connecticut School of Medicine and Dentistry

HHS Public Access

Author manuscript

J Immunol. Author manuscript; available in PMC 2017 June 01.

Published in final edited form as:

J Immunol. 2016 June 1; 196(11): 4510–4521. doi:10.4049/jimmunol.1600113.

TNF and CD28 signaling play unique but complementary roles in the systemic recruitment of innate immune cells after *Staphylococcus aureus* enterotoxin A inhalation[1]

Julia Svedova, **Naomi Tsurutani**[2], **Wenhai Liu**, **Kamal M. Khanna**, and **Anthony T. Vella**[3]

The Department of Immunology, School of Medicine, UConn Health, 263 Farmington Ave, Farmington CT

Abstract

Staphylococcus aureus enterotoxins cause debilitating systemic inflammatory responses, but how they spread systemically and trigger inflammatory cascade is unclear. Here, we showed in mice that after inhalation, *Staphylococcus aureus* enterotoxin A rapidly entered the bloodstream and induced T cells to orchestrate systemic recruitment of inflammatory monocytes and neutrophils. To study the mechanism used by specific T cells that mediate this process, a systems approach revealed inducible and non-inducible pathways as potential targets. It was found that TNF caused neutrophil entry into the peripheral blood, while CD28 signaling, but not TNF, was needed for chemotaxis of inflammatory monocytes into blood and lymphoid tissue. However, both pathways triggered local recruitment of neutrophils into lymph nodes. Thus, our findings revealed a dual mechanism of monocyte and neutrophil recruitment by T cells relying on overlapping and non-overlapping roles for the non-inducible costimulatory receptor CD28 and the inflammatory cytokine TNF. During sepsis, there might be clinical value in inhibiting CD28 signaling to decrease T cell-mediated inflammation and recruitment of innate cells while retaining bioactive TNF to foster neutrophil circulation.

Introduction

Staphylococcus aureus (*S. aureus*) is a part of normal human flora colonizing skin, nasopharynx and most commonly the anterior nares of the nose in almost 30% of the general population (1). A recent epidemiological study showed that Gram-positive bacteria were found in 47% of intensive care unit patients with an infection, with *S. aureus* present in 20% of positive cultures (2). Infection and related sepsis are one of the leading causes of death in the United States (3). Sepsis, characterized as systemic inflammatory response syndrome (SIRS) with a known or suspected infection, is a result of a dysregulated immune response, commonly accompanied by an uncontrolled release of cytokines that can lead to systemic

[1]The work was supported by NIAID P01AI056172 grant.

Address Correspondence: Anthony T. Vella, PhD., Department of Immunology, UConn Health, 263 Farmington Ave, Farmington, CT 06030.

[2]Current address: Wako Chemicals USA, Inc., 1600 Bellwood Road, Richmond, VA 23237

[3]Anthony T. Vella, PhD. Department of Immunology, School of Medicine, UConn Health, 263 Farmington Ave., Farmington, CT 06030. vella@uchc.edu

Conflict of Interest: The authors declare no conflicts of interest.

tissue injury, shock and even death (4). Methicillin-resistant *S. aureus* is particularly well spread in hospital settings and is associated with key virulence factors that may contribute to the severity and rapidity of sepsis (5). One such virulence factor is superantigens, such as *S. aureus* enterotoxins. These are heat resistant proteins that bypass classical antigen processing and presentation to mediate powerful oligoclonal T cell receptor Vβ chain-specific responses (6, 7) leading to toxic shock syndrome and potentially death (8–11).

A recent study showed that the presence of an enterotoxin was essential for the lethality of *S. aureus*-induced sepsis in rabbits (12). In addition, superantigens can synergize with TLR4 or TLR2 agonists and enhance the inflammatory response and the induction of lethal shock in mice (13, 14). Superantigens have been found in blood of septic patients and their prevalence, in particular prevalence of *S. aureus* enterotoxin A (SEA), was correlated with severity of infection (15–17). Therefore, it is likely that the presence of *S. aureus* enterotoxins drives or at least significantly exacerbates the inflammatory response in septic patients. It is still unclear, however, how *S. aureus* enterotoxins spread systemically especially in cases of an unknown entry point and how they trigger both adaptive and innate immunity to propagate systemic inflammation.

Mice exposed to *S. aureus* enterotoxins reproduce several important hallmarks of SIRS/sepsis in humans, including a rapid-onset immune response with a robust cytokine release (7, 18) and an immunosuppression/anergy phase (19–21) similar to the compensatory anti-inflammatory response syndrome (CARS) that often occurs in septic patients (22). Furthermore, SEA inhalation also recapitulates a common complication in sepsis, acute lung injury. The lungs of exposed mice show elevated proteins, presence of red blood cells and increased levels of cytokines (23, 24). Using the SEA model of SIRS, we sought to study systemic immune responses occurring immediately after SEA administration. The pulmonary SEA challenge resulted in a rapid release of monocytes and neutrophils to blood and their accumulation in lymphoid tissues. Remarkably, this inflammatory innate cell migration was dependent on the presence of T cells. In particular, the systemic recruitment of monocytes and neutrophils was dually regulated by T-cell based CD28 signaling and the inflammatory cytokine TNF.

Materials and Methods

Mice

C57BL/6J male mice and TCR $\beta\delta^{-/-}$ mice were obtained from Jackson Laboratory (Bar Harbor, Maine) and used between 6 and 16 weeks of age. All mice were kept in the Central Animal Facility at UConn Health in accordance with federal guidelines.

Immunization, therapy, and flow cytometry

Mice were immunized intranasally (i.n.) with 1 μg of SEA (Toxin Technology, Sarasota, FL) and the adaptive T cell transfer into TCR $\beta\delta^{-/-}$ mice were conducted as previously reported (23, 25). Specifically, ~3.5×10^6 C57BL/6J spleen and lymph nodes (LNs) nylon wool enriched T cells were transferred i.v. into TCR $\beta\delta^{-/-}$ mice.

For neutralization therapy experiments, mice received an i.p. injection of the following agents diluted in PBS: 200 μg of CTLA4-Ig or mouse IgG, 500 μg of anti-TNF (clone XT3.11) or rat IgG, 200 μg of anti-4-1BBL (clone TKS-1) or rat IgG_{2a}, anti-CD40L (clone MR1) or hamster IgG. Two hours later, they were challenged with SEA i.n. Blood and LNs were harvested 4 h after SEA inhalation. Murine CTLA4-Ig was a kind gift from Dr. Robert Mittler (Department of Surgery and Emory Vaccine Center, Emory University, Atlanta, GA). Mouse IgG was from Sigma-Aldrich (St. Louis, MO). The other antibodies and their isotype controls were obtained from Bio X Cell (Lebanon, NH).

For flow cytometry, the following fluorochrome-conjugated antibodies were used: anti-CD3 clone 145-2C11, anti-CD19 clone 1D3, anti-CD8a clone 53-6.7, B220 clone RA3-6B2, anti-NK1.1 clone PK136, anti-CD49b clone DX5, anti-Ly6G clone 1A8, anti-CD11c clone HL3, anti-Vβ3 clone KJ25, anti-Vβ14 clone 14-2, anti-CD25 clone PC61 (BD Biosciences, San Jose, CA), anti-Ly6C clone HK1.4, anti-CD11c clone N418, anti-MHC II clone M5/114.15.2, anti-CD69 clone H1.2F3, anti-CD103 clone 2E7 (eBioscience, San Diego, CA) and anti-CD11b clone M1/70 (BD Biosciences or eBioscience). Antibody-stained positive cells were determined with corresponding isotype controls. Live cell gate was determined using LIVE/DEAD® Fixable Blue Dead Cell Stain Kit (Life Technologies, Grand Island, NY). Surface staining for flow cytometry was performed as described previously (25). Briefly, LNs and spleen were crushed and passed through a 100-μm strainer (Falcon/BD Biosciences). Peripheral blood was collected into balanced salt solution (BSS) containing heparin (Sigma-Aldrich). Bone marrow (BM) was flushed out with BSS from one femur and tibia and passed through a 100-μm strainer. Spleen, BM and blood cells were treated with ammonium chloride solution to lyse RBCs. Single cell suspensions were counted with Z1 particle counter (Beckman Coulter, Brea, CA). Unspecific binding was blocked with FcR blocking solution (culture supernatant from 2.4.G.2 hybridoma, 5% mouse serum (Sigma-Aldrich), 10 μg/mL human IgG (Sigma-Aldrich), 0.1% sodium azide) and stained with antibodies and LIVE/DEAD stain for 30–45 min on ice. Flow cytometry was performed using a FACS-LSRII (BD Biosciences) and the data was analyzed with FlowJo software (Tree Star, Ashland, OR).

Cell sorting

For T cell sorting, LNs (cervical, mediastinal, axillary, brachial, inguinal, and mesenteric) were collected and processed as described above. For sorting of dendritic cells (DCs), the LN tissue was digested with collagenase solution (150 U/mL collagenase (Sigma-Aldrich), 2% FBS in MEM) for 30 min at 37°C and 5% CO_2. After tissue digestion, 100 μL of 0.1M EDTA in PBS per 1 mL of collagenase solution was added. The tissue was then passed through a 100-μm strainer and washed in 5 mM EDTA and 2% FBS Ca^{2+}/Mg^{2+} free BSS. After FcR blocking and antibody staining, cells were sorted with FACS Aria (BD Biosciences). The purity was typically ~98% (relative to live cells gate).

Co-culture assays

To obtain naïve T cells, spleen and LNs were harvested from a naïve mouse and processed as described above. To enrich the population of $Vβ3^+$ T cells, the cells were depleted using anti-B220 clone RA3-6B2, anti-NK1.1 clone PK136, anti-Vβ2 clone B20.6, anti-Vβ4 clone

KT-4, anti-Vβ5.1,5.2 clone MR9-4, anti-V6β clone RR4-7 and anti-Vβ8 clone F23.1 biotin-conjugated antibodies (eBioscience and BD Biosciences) and anti-biotin magnetic beads (Miltenyi Biotec Inc, Auburn, CA). For co-culture of T cells with serum or blood cells, tail blood was obtained 10 or 30 min after SEA or vehicle inhalation into either heparin-containing BSS or serum separator tubes (BD Biosciences). Blood cells were processed as described above. Next, the enriched T cells (100,000/well) were incubated with either cells derived from the blood (25,000/well) or the isolated serum (diluted 1:4 in culture medium) overnight at 37°C and 5% CO_2. For co-culture of T cells with DC subpopulations, LNs (mediastinal, cervical, axillary, brachial, inguinal) were collected 40 min after SEA or vehicle inhalation and processed as described above. The cells were enriched for DCs by depleting $B220^+$ and $Thy1.2^+$ cells using Dynabeads (Life Technologies), stained and sorted. The sorted DC subpopulations (5,000/well) were incubated with naïve enriched T cells (20,000/well) overnight at 37°C and 5% CO_2. After the culture, supernatants were collected to measure IL-2 concentration by ELISA (BD Biosciences) and the cells were washed and stained for flow cytometry as described above.

IL-6 ELISA and multiplex assay

To determine the level of IL-6 in serum, tail blood was collected into serum separator tubes (BD Biosciences). The isolated serum was stored at −80°C. IL-6 ELISA was conducted according to manufacturer's instruction (BD Biosciences). For the multiplex assay, LNs were isolated from mice 4 or 16 h after SEA or vehicle exposure. The tissue was placed in MagNA Lyser green beads tubes (Roche, Basel, Switzerland) filled with 400 μL PBS containing Protease Inhibitor Cocktail (Sigma-Aldrich) and lysed using MagNA Lyser Instrument (Roche) at 6,000 rpm for 1 min. The lysates were stored in −80°C. Chemokine and cytokine expressions were measured with customized Luminex®-based multiplex assay (EMD Millipore, Billerica, MA). The expression of individual chemokines and cytokines was normalized to the protein concentration measured by the Pierce BCA protein assay kit (Thermo Scientific, Rockford, IL).

Quantitative real-time PCR and RNA sequencing

For quantitative RT-PCR (qRT-PCR) analyses of the whole tissue, LNs from SEA or vehicle-exposed mice were removed, frozen on dry ice and stored at −80°C. To acquire RNA, the whole tissue was snap-frozen in liquid nitrogen and crushed into powder. The total RNA was isolated from the LN tissue or cells with RNeasy Mini Kit (Qiagen, Valencia, CA) and converted to cDNA using iScript cDNA Synthesis Kit (Biorad, Hercules, CA). mRNA expression level of target genes and the endogenous control gene *β-actin* were assessed by qRT-PCR using Taqman primers (Life Technologies) and a CFX96 RT-PCR instrument (Biorad). Each sample was run in duplicate and the gene expression was normalized to *β-actin* using the standard curve method.

For RNA sequencing, total LN cells (isolated from cervical, mediastinal, axillary, brachial, inguinal, and mesenteric LNs) were collected 40 min after SEA or vehicle inhalation. The cells were sorted and mRNA was acquired as described above. Total RNA was sequenced (Otogenetics, Norcross, GA) and transcriptomes from SEA $Vβ3^+$ T cells were compared to transcriptomes from vehicle $Vβ3^+$ T cells and SEA $Vβ14^+$ T cells(control groups). Genes in

SEA Vβ3$^+$ cells that were downregulated (log_2 fold change ≤ −1.5) or upregulated (log_2 fold change ≥ +1.5) compared to control groups in all three experiments were selected. The selected list of genes was further examined and any genes with inconsistent or close to zero expressions removed. Gene expressions patterns in the selected genes were analyzed using Gene set enrichment analysis (GSEA, Broad Institute, Cambridge, MA). The following gene set databases were used: h.all.v5.0.symbols.gmt and c5.all.v5.0.symbols.gmt (http://www.broadinstitute.org/gsea/msigdb/index.jsp). To construct heat maps, gene expressions were corrected to log_2 and processed using GENE-E software (Broad Institute). The RNA sequencing data can be viewed online (http://www.ncbi.nlm.nih.gov/geo/; accession number: GSE76190).

Confocal microscopy

Whole LN tissue was fixed in periodate-lysine-paraformaldehyde solution (1 μM sodium periodate, 75 mM L-lysine, 1% paraformaldehyde in phosphate buffer) at 4°C overnight. The LNs were washed in phosphate buffer and left in 30% sucrose at 4°C overnight. The tissue was frozen in OCT and stored at −80°C. The frozen tissue was cut into 20 μm-thick sections with LEICA CM1850 cryostat (Leica Biosystems, Buffalo Grove, IL) and the sections were stored at −20°C. For antibody staining, the sections were firstly blocked for unspecific binding using a staining buffer (either 2% FBS in PBS or 2% FBS, 2% goat serum, 0.5% FcR blocking solution, 0.05% Tween-20, 0.3% Tritone-X100 in PBS) for 1 h at room temperature and then stained with primary antibodies diluted in the staining buffer for 1 h at room temperature. The sections were examined with Zeiss LSM780 confocal microscope (Zeiss, Oberkochen, Germany). Inflammatory innate immune cells were identified by V450-conjugated anti-CD11b clone M1/70 (BD Biosciences) and DyLight 488-conjugated anti-Ly6B.2 clone 7/4 (labeled as 7/4; Novus Biologicals, Littleton, CO). B cell follicles were determined with Pacitic Orange-conjugated anti-B220 clone RA3-6B2 (Life Technologies). The images represent confocal z-stack projections, which were acquired using 20×/0.8 numerical aperture objective. Image analysis, including adjustment for contrast and brightness and cellular quantification, was done with Imaris software (Bitplane, Zurich, Switzerland).

Statistical analysis

The two-tailed Student's unpaired *t*-test was used to evaluate statistical significance ($P<0.05$). All statistical tests were performed using Prism-GraphPad (La Jolla, CA) and Microsoft Excel.

Results

Systemic recruitment of monocytes and neutrophils is observed rapidly after SEA inhalation

SEA inhalation results in alveolitis characterized by increased protein content, presence of RBCs, secretion of cytokines, and accumulation of monocytes and neutrophils (23, 25). The local lung response is coincident with an expansion of SEA-specific T cells in all lymphoid tissues (23). To understand how SEA inhalation causes a systemic response, serum and blood cells were isolated immediately after SEA or vehicle challenge and incubated with

enriched naïve T cells. Cells derived from blood after SEA or vehicle inhalation and serum from vehicle mice did not affect T cell activation (Fig 1A and B; data not shown). However, serum obtained only 10 min after SEA inhalation was able to activate SEA-specific $V\beta3^+$ T cells to express CD69 and CD25 while having little effect on bystander $V\beta14^+$ T cells (Fig 1A and B). The same type of response was observed when the naïve T cells were incubated with SEA (data not shown). Finally, only T cells co-cultured with serum from SEA mice produced IL-2 (Fig. 1C). Thus, SEA can rapidly enter the bloodstream after inhalation in sufficient quantities to activate T cells.

The rapid spread of the enterotoxin after inhalation through blood posed the question of whether the systemic inflammatory response to SEA was accompanied by a common hallmark of SIRS and sepsis, blood leukocytosis (4). To test if SEA inhalation mediates systemic circulation of innate immune cells, mice were challenged with SEA or vehicle alone and then the peripheral blood cells were analyzed for the presence of monocytes or neutrophils. Inflammatory monocytes were identified as $CD3^-CD19^-CD11b^+Ly6G^-Ly6C^{hi}$ while neutrophils were identified as $CD3^-CD19^-CD11b^+Ly6G^+Ly6C^+$ (Suppl. Fig. 1A). The percent of neutrophils in blood increased 6.4-fold 2 h after SEA challenge compared to vehicle while there was no relative increase in monocytes (Fig. 2A). Nevertheless, both populations were increased 4 h after SEA inhalation. SEA-based inflammation is dependent on T cells, which are found in lymphoid tissues (23). Therefore, it was hypothesized that the circulating inflammatory innate cells would migrate to the LNs and spleen. Indeed, the percent of inflammatory monocytes and neutrophils at 4 h after SEA inhalation was increased in spleen, mediastinal, cervical, and non-draining LNs compared to vehicle control (Fig. 2B). Inflammatory monocytes remained elevated at 12 h whereas the percent of neutrophils decreased to the level of vehicle-treated mice. Like percentages, the same trends were observed when assessing the absolute numbers of inflammatory monocytes and neutrophils (Suppl. Fig. 1B). The recruited monocytes likely originated from the BM because there was a depletion of BM inflammatory monocytes reaching over 50% reduction compared to the vehicle control by 4 h after SEA inhalation (Fig. 2C). Interestingly, SEA challenge caused only a small decline in the number of BM neutrophils. In sum, SEA inhalation resulted in rapid systemic recruitment of monocytes and neutrophils to blood and lymphoid tissues.

The recruitment of innate immune cells after SEA inhalation is guided by T cells to the T cell zone of the LNs

SEA inhalation induces monocyte and neutrophil migration to lungs in a T cell dependent manner (25). To determine the role of T cells in the systemic recruitment of innate immune cells to blood and LNs, TCR $\beta\delta^{-/-}$ mice, that lack both $\alpha\beta$ and $\gamma\delta$ T cells, received C57BL/6J T cells or nothing and subsequently, they were i.n. challenged with SEA or vehicle. In the absence of T cell transfer, cervical LNs and blood from SEA-treated mice showed no difference in accumulation of monocytes or neutrophils compared to the vehicle group (Fig. 3). However, SEA-challenged TCR $\beta\delta^{-/-}$ mice that received T cells had significant increases in the percent of both monocytes and neutrophils compared to vehicle alone (Fig. 3). Thus, T cells were required to trigger the systemic recruitment of inflammatory innate immune cells to blood and LNs after inhalation of SEA.

Migration of neutrophils and monocytes to LNs was previously reported (26–32). However, while some studies showed that following an infection or antigen challenge, neutrophils were recruited to the subcapsular sinus (26, 29), others found innate immune cells in the T cell zone (30, 32). To determine where the recruited cells accumulated, cervical LNs were collected 1, 2, and 4 h after SEA inhalation and examined by confocal microscopy. Inflammatory innate immune cells ($CD11b^+7/4^+$) were detected in the LNs as early as 2 h after SEA but not in the vehicle control (Fig. 4A). By 4 h, the quantity of inflammatory innate immune cells increased even further, which was confirmed by enumerating $7/4^+$ cells per field (Fig. 4B). Importantly, the recruited cells were primarily in the T cell zone of the LNs whereas the few inflammatory cells in the vehicle alone mice were mostly located in the subcapsular sinus and B cell follicles (Fig. 4C). These findings demonstrate that SEA inhalation induced recruitment of monocytes and neutrophils particularly to the T cell zone in the LNs where the SEA-specific T cells become activated.

SEA inhalation triggers a rapid release of specific chemokines by both T cells and dendritic cells

Monocyte and neutrophil migration can be driven by a number of chemokines (33–35). To understand which chemotactic factors might play a role in the systemic recruitment of monocytes and neutrophils, total RNA was isolated from draining LNs (cervical and mediastinal) to assess the expression of various chemokine genes. Compared to vehicle, expression of multiple chemotactic factors increased as early as 1 h after SEA inhalation (Suppl. Fig. 2A). Interestingly, mRNA levels of chemokines particularly important for the recruitment of neutrophils and monocytes – *Cxcl1*, *Cxcl2*, *Ccl2*, *Ccl3*, *Ccl4*, and *Ccl7* (33, 35) showed a rapid increase in expression peaking at 2 h (Suppl. Fig. 2A; clear bar graphs). To validate these findings, LN lysates were examined for the protein levels of these chemokines by a multiplex assay. Multiple chemokines were significantly elevated 4 h after SEA inhalation, including 38-fold for CXCL1, 792-fold for CXCL2, 53-fold for CCL2, 46-fold for CCL3 and 92-fold for CCL4 (Suppl. Fig. 2B). Nevertheless, the increased chemokine levels were transient because by 16 h after SEA challenge, they were already decreasing. In addition, the expression of chemotactic factors was systemic as SEA challenge caused a similar increase in chemokine levels in draining LNs, peripheral LNs, and mesenteric LNs (data not shown). We previously showed that SEA-activated αβ T cells directed γδ T cells to release IL-17, which contributed to the recruitment of neutrophils to lungs after SEA inhalation (25). Therefore, we assayed for IL-17, but only a small increase was detected in the LN lysates of the SEA group compared to vehicle (Suppl. Fig. 2B, bottom panel).

Because SEA can directly crosslink MHC class II (MHC II) molecules on antigen-presenting cells and Vβ chains of the TCR (36), we hypothesized that DCs and T cells were an important source of chemokines recruiting monocytes and neutrophils. Therefore, $Lin^-CD11c^+MHC\ II^+$ DCs were sorted and the relative expression of chemokines was determined. DCs from SEA-challenged mice upregulated *Cxcl1* and *Cxcl2* mRNA levels but not *Ccl3* and *Ccl4* compared to DCs from the vehicle group (Fig. 5A). Interestingly, SEA-activated $V\beta3^+$ T cells but not bystander $V\beta14^+$ T cells substantially expressed *Ccl3* and *Ccl4*, in particular, 680-fold and 738-fold increases compared to vehicle, respectively (Fig.

5B). DCs are heterogeneous and thus, to understand if a specific subset was critical, $CD11c^{low}$MHC II^{hi} migratory DCs and $CD11c^{hi}$MHC II^{low} resident DCs (37, 38) were sorted (Fig. 5C). Migratory DCs expressed more *Cxcl1* and *Cxcl2* as normalized to *β-actin* expression than the resident DCs (Fig. 5D). To summarize, SEA inhalation induced rapid production of chemokines by SEA-activated T cells and DCs (predominatly migratory DCs).

To see if the differential chemokine expression in the DC subpopulations was due to their ability to present SEA, we tested if either migratory DC ($Lin^{-}CD11c^{low}$MHC II^{hi}) or resident DC ($Lin^{-}CD11c^{hi}$MHC II^{low}) subpopulations were preferentially stimulating the SEA-specific T cells. In particular, four distinct DC subpopulations were sorted from either SEA or vehicle-immunized mice (Fig. 6A) and without adding SEA, the sorted DC subpopulations were cultured with naïve T cells. Both $CD11b^{+}$ and $CD103^{+}$ migratory DCs from the SEA-immunized mice, but not resident DCs, activated $V\beta3^{+}$ T cells to upregulate CD69 (Fig. 6B). There was no difference in CD69 expression on the bystander $V\beta14^{+}$ T cells when cultured with DCs from SEA-immunized mice compared to the vehicle control. These findings show that that only migratory DCs presented SEA *ex vivo* to naïve SEA-specific T cells.

Mechanism of T cell guided innate cell recruitment

To determine the mechanism of how SEA-activated T cells promote chemokine production by DCs, SEA-specific $V\beta3^{+}$ and bystander $V\beta14^{+}$ T cells were sorted 40 min after SEA or vehicle inhalation and RNA was isolated for transcriptome analysis (Suppl. Fig. 3A). Comparing RNA from SEA $V\beta3^{+}$ T cells to vehicle $V\beta3^{+}$ or SEA $V\beta14^{+}$ control groups, many genes were found to be upregulated in the SEA-specific $V\beta3^{+}$ T cells (Suppl. Fig. 3B). Gene expression increases were predominantly associated with cell development, proliferation, and regulation of metabolic processes. However, GSEA also revealed a significant association with apoptosis and negative regulation of cells (Suppl. Fig. 3C). In addition, both pro- (*Tnf*, *Il2*, *Ifng*) and anti-inflammatory cytokines (*Il10*) were upregulated in $V\beta3^{+}$ T cells from the SEA-treated group suggesting a role for T cell costimulation (Suppl. Fig. 3D).

The expression of inducible as well as constitutively expressed costimulatory molecules were compared. While there was no difference in the expression of constitutively expressed costimulatory molecules, five inducible costimulatory molecules were significantly upregulated in SEA $V\beta3^{+}$ T cells, including 4-1BBL (*Tnfsf9*), LIGHT (*Tnfsf14*), CD40L (*Cd40lg*), SLAM (*Slamf1*), and TWEAK receptor (*Tnfrsf12a*) (Fig. 6C and D). Interestingly, inducible coinhibitory molecules, particularly PD-L1 (*Cd274*), PD-L2 (*Pdcd1lg2*), and PD1 (*Pdcd1*), were also upregulated in SEA $V\beta3^{+}$ T cells compared to the control groups (Suppl. Fig. 3E and F), further confirming the dual capacity of T cells to promote and suppress inflammation immediately after SEA inhalation.

Previous studies found that 4-1BB-4-1BBL and CD40-CD40L pathways can enhance the recruitment of innate immune cells (39, 40). Furthermore, 4-1BBL and CD40L expression on $V\beta3^{+}$ T cells was validated by flow cytometry (data not shown). Therefore, it was hypothesized that the systemic migration of innate immune cells might be dependent on the expression of inducible costimulatory molecules. To determine whether 4-1BBL and CD40L

play a role in the migration of monocytes and neutrophils, mice were pre-treated with anti-4-1BBL, anti-CD40L or the corresponding IgG control and then i.n. challenged with SEA. Neither 4-1BBL nor CD40L blockade impeded migration of monocytes or neutrophils to blood and LNs (Suppl. Fig. 4A and B), suggesting other mechanisms were involved.

One possibility is that a constitutively expressed costimulatory molecule, such as CD28, might be responsible for this recruitment. The membrane receptor CD28 engages its ligands CD80 and CD86 on DCs and potently enhances TCR-induced cytokine release and proliferation of naïve T cells (41, 42). In addition, CD28 engagement is needed for optimal superantigen-induced T cell expansion (43). Consistent with this previous work, genes associated with CD28 signaling (44–46) were upregulated in $V\beta3^+$ T cells after SEA inhalation (data not shown). Secondly, cytokines like TNF and IL-2 are major factors released by enterotoxin-specific T cells (11, 47) and our data show that *Tnf* is promptly synthesized by SEA-specific $V\beta3^+$ T cells (Suppl Fig. 3D). Furthermore, GSEA of the hallmark pathways demonstrated a significant enrichment in the pathway of TNF signaling via NFκB in the SEA-specific $V\beta3^+$ T cells (Fig. 7A). Thus, it was hypothesized that CD28 costimulation and a cytokine played redundant or non-overlapping roles in innate cell recruitment in SEA-triggered acute inflammation.

To test this notion, CD28 and TNF were neutralized in SEA-treated mice with CTLA4-Ig or anti-TNF. First, we tested whether CD28 or TNF neutralization affected serum IL-6 levels since increased IL-6 correlates with decreased survival not only in models of sepsis but also in septic patients (48–51). Both, CTLA4-Ig and anti-TNF significantly reduced serum IL-6 compared to the IgG controls, with anti-TNF being even more effective in decreasing IL-6 than CTLA4-Ig (Fig. 7B). Thus, both treatments appeared to attenuate inflammation by reducing serum IL-6 levels.

To assess whether CD28 or TNF orchestrate monocyte and neutrophil chemotaxis after SEA inhalation, LN tissue from CTLA4-Ig or anti-TNF treated-mice was examined for the expression of chemokines. While CTLA4-Ig significantly reduced *Cxcl1*, *Cxcl2*, *Ccl2*, *Ccl3*, and *Ccl7* mRNA expression, anti-TNF only decreased *Cxcl2* expression and had no significant effect on the other chemokines (Fig. 7C). These findings suggested that CTLA4-Ig would be more effective in blocking the systemic recruitment of monocytes and neutrophils compared to anti-TNF. Indeed, the percent of inflammatory monocytes in LNs and blood was significantly reduced after CTLA4-Ig treatment. In contrast, anti-TNF relatively increased the percent of monocytes in the blood but had no effect on their migration to LNs (Fig. 7D). Nevertheless, both CD28 and TNF blockade significantly reduced the accumulation of neutrophils in LNs (Fig. 7E, upper panels). Based on the results from Fig. 1A, which demonstrated robust migration of neutrophils and monocytes into the bloodstream after SEA inhalation, it was tested if these pathways operated by preventing migration of innate cells into blood. CTLA4-Ig did not inhibit neutrophil circulation (Fig. 7E, lower left panel), but interestingly, TNF blockade significantly inhibited recruitment of neutrophils into blood (Fig. 7E, lower right panel). These findings posed the question of whether the reduction of neutrophils in the LNs after anti-TNF treatment was due to the decreased circulation of blood neutrophils (Fig 7E, lower panels) or reduced *Cxcl2* expression (Fig. 7C). In TNF blocked mice, there was no correlation between the percentage

of neutrophils in the blood versus the LNs (Fig. 7F). However, mRNA *Cxcl2* expression positively correlated with the percentage of neutrophils in the LNs suggesting that migration into LNs was dependent on a chemokine gradient rather than the amount of circulating cells (Fig. 7G). Thus, the systemic recruitment of monocytes and neutrophils after SEA inhalation is orchestrated by a non-inducible CD28 signal with overlapping and non-overlapping roles for TNF.

Discussion

Staphylococcus aureus enterotoxins have been implicated in the pathology of toxic shock, sepsis as well as a number of pulmonary and autoimmune diseases due to their ability to elicit a massive and systemic cytokine storm (18, 52–54). However, it is unclear how *S. aureus* enterotoxins enter the periphery to instigate these effects since the lungs and airways are usually impermeable to inhaled antigens. In fact, antigens are typically cleared from these tissues by a number of mechanisms, including mucociliary transport, innate defense molecules and resident phagocytes (55, 56). Alternatively, inhaled antigens can be carried by migratory DCs to the draining LNs where they are presented to antigen-specific T cells, a process that occurs over hours (55, 57). Unlike most antigens, we demonstrate in this report that inhaled SEA enters the blood circulation within minutes and can be recovered in the serum rather than associated with cells (Fig. 1). This ability to enter the bloodstream while maintaining its full bioactivity accounts for the rapid systemic response observed after *S. aureus* enterotoxin pulmonary exposure (23, 25).

From a biomedical perspective, our study showed that just as seen in many patients with SIRS/sepsis (58), SEA inhalation induced leukocytosis since the pulmonary SEA challenge initiated rapid recruitment of innate immune cells to blood followed by their migration to lymphoid tissues (Fig. 2). During inflammation, innate immune cells are often assumed to originate from BM. While the pool of inflammatory monocytes in the BM was markedly depleted, there was only a small decrease in BM neutrophils after SEA inhalation (Fig. 2C). A second neutrophil reservoir is the marginated pool where the egress of neutrophils is much faster than the BM peaking at 2 h after an injection of a stimulant (59). The large increase in circulating neutrophils 2 h after SEA inhalation suggests that many of the recruited neutrophils originated from the marginated pool rather than BM.

Activation and expansion of T cells has been considered the core of *S. aureus* enterotoxin-induced inflammation (18). Nevertheless, several studies reported that an inflammatory response could occur even in the absence of T cells (60, 61). In the inhaled SEA model of SIRS, TCR $\beta\delta^{-/-}$ mice were unable to recruit monocytes and neutrophils to blood and LNs whereas only a small transfer of T cells induced a rapid mobilization of the innate cells (Fig. 3). The recruited cells localized to the T cell zone of the LNs (Fig. 4). This specific location in the LNs renders an opportunity to modulate adaptive immunity. Previous studies showed that after recruitment to LNs, inflammatory monocytes differentiate into DCs and are capable of antigen presentation, including cross-presentation, resulting in enhanced Th1 responses via IL-12 (31, 32). Similarly, neutrophil migration to LNs has been associated with several different functions, including carrying bacteria to LNs via the lymphatic system, augmenting lymphocyte proliferation, and downregulating CD4 T cell responses by

decreasing antigen presentation by antigen-presenting cells (27, 29, 62). Thus, it will be important to determine if the migration of inflammatory monocytes and neutrophils to the T cell zone of LNs affects the function of T cells and the overall inflammatory response after pulmonary *S. aureus* enterotoxin challenge.

To test whether the recruitment of innate immune cells was caused by mediators directly released by T cells, we examined T cells for chemokine expression and found that upon activation, T cells expressed chemokines but also induced chemokine expression in DCs (Fig. 5). This was coincident with increases in inducible costimulatory pathways rapidly after SEA inhalation that included *Tnfsf9* (4-1BBL) and *Cd40lg* (CD40L) (Fig. 6C and D). However, while inducible costimulation was not involved in the monocyte and neutrophil chemotaxis (Suppl. Fig. 4), blocking non-inducible CD28 costimulation significantly reduced the migration of inflammatory monocytes (Fig. 7D). In contrast, neutrophil recruitment was driven by two T cell-dependent signals. Firstly, TNF triggered a rapid release of neutrophils into blood, which we postulate is derived from the marginated pool. Secondly, a chemokine axis induced by both the CD28 and TNF pathways directed neutrophils to LNs (Fig. 7E). In particular, the inhibition of neutrophil migration to LNs was coincident with reduced expression of *Cxcl2* (Fig. 7C and D) and it was previously reported that the migration of neutrophils into tumor-draining LNs via high endothelial venules was dependent on CXCL2 but not on CXCL1 (30). Therefore, we hypothesize that CXCL2 may be the key chemokine driving the neutrophil migration into LNs from blood after pulmonary challenge with *S. aureus* enterotoxins or during Gram-positive sepsis. Finally, we showed that T cells were essential for the systemic recruitment of neutrophils and monocytes after SEA inhalation (Fig. 3). However, because TNF can be produced by many cell types (63) and CD28 expression was reported on immune cells other than T cells (64, 65), it is possible that blocking with CTLA4-Ig and anti-TNF affected other cell populations that could also contribute to the reduced migration of innate cells.

Despite decades of research, there is currently no approved drug treatment for SIRS/sepsis patients (4). Because of the central role TNF plays in the pathology of SIRS/sepsis, anti-TNF therapies were previously thought to be an excellent therapeutic target (66). However, clinical studies failed to find improvements in the outcomes of patients with sepsis receiving anti-TNF treatment (67–69). Moreover, rheumatoid arthritis patients on anti-TNF therapy gained a higher likelihood of developing serious infections (70). Our results show that although TNF blockade attenuated inflammation by reducing serum IL-6 (Fig. 7B), it also significantly depleted the pool of circulating blood neutrophils (Fig. 7E). The capacity of neutrophils to mount a rapid microbicidal response makes them a crucial component of the immune system during sepsis. In fact, the relative resistance to *S. aureus* in C57BL/6 mice was recently attributed to increased chemokine secretion and subsequent neutrophil recruitment compared to other mouse strains (71). In addition, reduced levels of circulating neutrophils may be associated with a decreased likelihood of survival in sepsis (48, 72). The suppressed neutrophil levels in blood could potentially compromise the immune system's capacity to kill off bacteria in the bloodstream. Therefore, it is possible that the failure of anti-TNF therapies to ameliorate outcomes in sepsis is partially due to the reduced neutrophil count in blood leading to increased bacteremia.

Costimulatory molecules represent another group of potential therapeutic targets in SIRS/sepsis. In particular, CD28 may play an important role in the propagation of inflammation during the course of the disease. A clinical trial using a monoclonal superagonist anti-CD28 resulted in a life-threatening SIRS with clinical signs and symptoms similar to sepsis (73). In contrast, blocking CD28 signaling, especially in cases of superantigen-induced toxic shock, showed attenuation of the disease in mice (74, 75). Here we showed that blocking CD28 reduced IL-6 levels and chemokine expression, while impeding migration of monocytes and neutrophils to LNs without affecting neutrophilia in blood (Fig. 7). Therefore, targeting CD28, especially in cases of Gram-positive sepsis in which *S. aureus* enterotoxins may drive the pathology, merits further investigation.

Lastly, not only costimulatory but also coinhibitory molecules, particularly *Cd274* (PD-L1), *Pdcd1lg2* (PD-L2) and *Pdcd1* (PD1), were upregulated after SEA inhalation (Suppl. Fig. 3). Similarly, both pro- and anti-inflammatory cytokines were upregulated as were the processes of cell activation and apoptosis (Suppl. Fig. 3). In patients with sepsis, the acute SIRS phase characterized by a hyperinflammatory state and the release of pro-inflammatory cytokines was thought to be frequently followed by an immunosuppressive CARS phase and presence of anti-inflammatory cytokines (76). However, recent evidence suggests that both pro- and anti-inflammatory responses occur simultaneously from the onset of sepsis with one prevailing over the other during the course of the disease (4, 77, 78). Similarly, we showed that both inflammatory and immunosuppressive processes are triggered simultaneously in T cells immediately after SEA inhalation, confirming the relevance of *S. aureus* enterotoxins in the pathology of sepsis.

In sum, our study demonstrated that inhaled SEA rapidly enters the bloodstream and triggers systemic inflammation by forming an inflammatory cell network comprised of both the innate and adaptive immune system. In particular, our findings revealed a dual mechanism of monocyte and neutrophil recruitment by SEA-specific T cells relying on overlapping and non-overlapping roles of the non-inducible costimulatory receptor CD28 and the inflammatory cytokine TNF. Treatments for SIRS/sepsis may benefit by targeting disease initiation rather than treating the consequent symptoms.

Supplementary Material

Refer to Web version on PubMed Central for supplementary material.

Acknowledgments

We would like to thank Dr. Adam Adler for reviewing the manuscript and Dr. Antoine Ménoret for his assistance during data collection.

Abbreviations used in this article

S. aureus	*Staphylococcus aureus*
SIRS	systemic inflammatory response syndrome
SEA	*S. aureus* enterotoxin A

CARS	compensatory anti-inflammatory response syndrome
LN	lymph node
i.n	intranasally
BSS	balanced salt solution
BM	bone marrow
DC	dendritic cell
qRT-PCR	quantitative RT-PCR
GSEA	gene set enrichment analysis
MHC II	MHC class II
cDC	conventional DC

References

1. Wertheim HF, Melles DC, Vos MC, van Leeuwen W, van Belkum A, Verbrugh HA, Nouwen JL. The role of nasal carriage in Staphylococcus aureus infections. Lancet Infect Dis. 2005; 5:751–762. [PubMed: 16310147]
2. Vincent JL, Rello J, Marshall J, Silva E, Anzueto A, Martin CD, Moreno R, Lipman J, Gomersall C, Sakr Y, Reinhart K. International study of the prevalence and outcomes of infection in intensive care units. JAMA. 2009; 302:2323–2329. [PubMed: 19952319]
3. Murphy, SL.; Kochanek, KD.; Xu, J.; Heron, M. National Vital Statistics Reports. National Center for Health Statistics; Hyattsville, MD: 2015. Deaths: Final Data for 2012.
4. Iskander KN, Osuchowski MF, Stearns-Kurosawa DJ, Kurosawa S, Stepien D, Valentine C, Remick DG. Sepsis: multiple abnormalities, heterogeneous responses, and evolving understanding. Physiol Rev. 2013; 93:1247–1288. [PubMed: 23899564]
5. Naber CK. Staphylococcus aureus bacteremia: epidemiology, pathophysiology, and management strategies. Clin Infect Dis. 2009; 48(Suppl 4):S231–237. [PubMed: 19374578]
6. Fields BA, Malchiodi EL, Li H, Ysern X, Stauffacher CV, Schlievert PM, Karjalainen K, Mariuzza RA. Crystal structure of a T-cell receptor beta-chain complexed with a superantigen. Nature. 1996; 384:188–192. [PubMed: 8906797]
7. Li H, Llera A, Malchiodi EL, Mariuzza RA. The structural basis of T cell activation by superantigens. Annu Rev Immunol. 1999; 17:435–466. [PubMed: 10358765]
8. Arad G, Levy R, Hillman D, Kaempfer R. Superantigen antagonist protects against lethal shock and defines a new domain for T-cell activation. Nat Med. 2000; 6:414–421. [PubMed: 10742148]
9. Schlievert PM. Role of superantigens in human disease. J Infect Dis. 1993; 167:997–1002. [PubMed: 8486972]
10. Kotzin BL, Leung DY, Kappler J, Marrack P. Superantigens and their potential role in human disease. Adv Immunol. 1993; 54:99–166. [PubMed: 8397479]
11. Miethke T, Wahl C, Heeg K, Echtenacher B, Krammer PH, Wagner H. T cell-mediated lethal shock triggered in mice by the superantigen staphylococcal enterotoxin B: critical role of tumor necrosis factor. J Exp Med. 1992; 175:91–98. [PubMed: 1730929]
12. Salgado-Pabon W, Breshears L, Spaulding AR, Merriman JA, Stach CS, Horswill AR, Peterson ML, Schlievert PM. Superantigens are critical for Staphylococcus aureus Infective endocarditis, sepsis, and acute kidney injury. MBio. 2013; 4:e00494–00413. [PubMed: 23963178]
13. Blank C, Luz A, Bendigs S, Erdmann A, Wagner H, Heeg K. Superantigen and endotoxin synergize in the induction of lethal shock. Eur J Immunol. 1997; 27:825–833. [PubMed: 9130631]

14. Kearney DE, Wang W, Redmond HP, Wang JH. Bacterial superantigens enhance the in vitro proinflammatory response and in vivo lethality of the TLR2 agonist bacterial lipoprotein. J Immunol. 2011; 187:5363–5369. [PubMed: 22003201]
15. Azuma K, Koike K, Kobayashi T, Mochizuki T, Mashiko K, Yamamoto Y. Detection of circulating superantigens in an intensive care unit population. Int J Infect Dis. 2004; 8:292–298. [PubMed: 15325598]
16. Desachy A, Lina G, Vignon P, Hashemzadeh A, Denis F, Etienne J, Francois B, Ploy MC. Role of superantigenic strains in the prognosis of community-acquired methicillin-susceptible Staphylococcus aureus bacteraemia. Clin Microbiol Infect. 2007; 13:1131–1133. [PubMed: 17727671]
17. Ferry T, Thomas D, Genestier AL, Bes M, Lina G, Vandenesch F, Etienne J. Comparative prevalence of superantigen genes in Staphylococcus aureus isolates causing sepsis with and without septic shock. Clin Infect Dis. 2005; 41:771–777. [PubMed: 16107972]
18. Fraser JD, Proft T. The bacterial superantigen and superantigen-like proteins. Immunol Rev. 2008; 225:226–243. [PubMed: 18837785]
19. Kawabe Y, Ochi A. Selective anergy of V beta 8+,CD4+ T cells in Staphylococcus enterotoxin B-primed mice. J Exp Med. 1990; 172:1065–1070. [PubMed: 1976734]
20. Rellahan BL, Jones LA, Kruisbeek AM, Fry AM, Matis LA. In vivo induction of anergy in peripheral V beta 8+ T cells by staphylococcal enterotoxin B. J Exp Med. 1990; 172:1091–1100. [PubMed: 2212944]
21. Cauley LS, Cauley KA, Shub F, Huston G, Swain SL. Transferable anergy: superantigen treatment induces CD4+ T cell tolerance that is reversible and requires CD4-CD8- cells and interferon gamma. J Exp Med. 1997; 186:71–81. [PubMed: 9206999]
22. Ward NS, Casserly B, Ayala A. The compensatory anti-inflammatory response syndrome (CARS) in critically ill patients. Clin Chest Med. 2008; 29:617–625. viii. [PubMed: 18954697]
23. Muralimohan G, Rossi RJ, Guernsey LA, Thrall RS, Vella AT. Inhalation of Staphylococcus aureus enterotoxin A induces IFN-gamma and CD8 T cell-dependent airway and interstitial lung pathology in mice. J Immunol. 2008; 181:3698–3705. [PubMed: 18714046]
24. Menoret A, Kumar S, Vella AT. Cytochrome b5 and cytokeratin 17 are biomarkers in bronchoalveolar fluid signifying onset of acute lung injury. PLoS One. 2012; 7:e40184. [PubMed: 22792238]
25. Kumar S, Colpitts SL, Menoret A, Budelsky AL, Lefrancois L, Vella AT. Rapid alphabeta T-cell responses orchestrate innate immunity in response to Staphylococcal enterotoxin A. Mucosal Immunol. 2013; 6:1006–1015. [PubMed: 23321986]
26. Chtanova T, Schaeffer M, Han SJ, van Dooren GG, Nollmann M, Herzmark P, Chan SW, Satija H, Camfield K, Aaron H, Striepen B, Robey EA. Dynamics of neutrophil migration in lymph nodes during infection. Immunity. 2008; 29:487–496. [PubMed: 18718768]
27. Abadie V, Badell E, Douillard P, Ensergueix D, Leenen PJ, Tanguy M, Fiette L, Saeland S, Gicquel B, Winter N. Neutrophils rapidly migrate via lymphatics after Mycobacterium bovis BCG intradermal vaccination and shuttle live bacilli to the draining lymph nodes. Blood. 2005; 106:1843–1850. [PubMed: 15886329]
28. Gorlino CV, Ranocchia RP, Harman MF, Garcia IA, Crespo MI, Moron G, Maletto BA, Pistoresi-Palencia MC. Neutrophils exhibit differential requirements for homing molecules in their lymphatic and blood trafficking into draining lymph nodes. J Immunol. 2014; 193:1966–1974. [PubMed: 25015824]
29. Yang CW, Strong BS, Miller MJ, Unanue ER. Neutrophils influence the level of antigen presentation during the immune response to protein antigens in adjuvants. J Immunol. 2010; 185:2927–2934. [PubMed: 20679530]
30. Brackett CM, Muhitch JB, Evans SS, Gollnick SO. IL-17 promotes neutrophil entry into tumor-draining lymph nodes following induction of sterile inflammation. J Immunol. 2013; 191:4348–4357. [PubMed: 24026079]
31. Nakano H, Lin KL, Yanagita M, Charbonneau C, Cook DN, Kakiuchi T, Gunn MD. Blood-derived inflammatory dendritic cells in lymph nodes stimulate acute T helper type 1 immune responses. Nat Immunol. 2009; 10:394–402. [PubMed: 19252492]

32. Cheong C, Matos I, Choi JH, Dandamudi DB, Shrestha E, Longhi MP, Jeffrey KL, Anthony RM, Kluger C, Nchinda G, Koh H, Rodriguez A, Idoyaga J, Pack M, Velinzon K, Park CG, Steinman RM. Microbial stimulation fully differentiates monocytes to DC-SIGN/CD209(+) dendritic cells for immune T cell areas. Cell. 2010; 143:416–429. [PubMed: 21029863]
33. Sadik CD, Kim ND, Luster AD. Neutrophils cascading their way to inflammation. Trends Immunol. 2011; 32:452–460. [PubMed: 21839682]
34. Williams AE, Chambers RC. The mercurial nature of neutrophils: still an enigma in ARDS? Am J Physiol Lung Cell Mol Physiol. 2014; 306:L217–230. [PubMed: 24318116]
35. Shi C, Pamer EG. Monocyte recruitment during infection and inflammation. Nat Rev Immunol. 2011; 11:762–774. [PubMed: 21984070]
36. Herman A, Kappler JW, Marrack P, Pullen AM. Superantigens: mechanism of T-cell stimulation and role in immune responses. Annu Rev Immunol. 1991; 9:745–772. [PubMed: 1832875]
37. Anandasabapathy N, Feder R, Mollah S, Tse SW, Longhi MP, Mehandru S, Matos I, Cheong C, Ruane D, Brane L, Teixeira A, Dobrin J, Mizenina O, Park CG, Meredith M, Clausen BE, Nussenzweig MC, Steinman RM. Classical Flt3L-dependent dendritic cells control immunity to protein vaccine. J Exp Med. 2014; 211:1875–1891. [PubMed: 25135299]
38. Cerny D, Haniffa M, Shin A, Bigliardi P, Tan BK, Lee B, Poidinger M, Tan EY, Ginhoux F, Fink K. Selective susceptibility of human skin antigen presenting cells to productive dengue virus infection. PLoS Pathog. 2014; 10:e1004548. [PubMed: 25474532]
39. Lee SC, Ju SA, Sung BH, Heo SK, Cho HR, Lee EA, Kim JD, Lee IH, Park SM, Nguyen QT, Suh JH, Kim BS. Stimulation of the molecule 4-1BB enhances host defense against Listeria monocytogenes infection in mice by inducing rapid infiltration and activation of neutrophils and monocytes. Infect Immun. 2009; 77:2168–2176. [PubMed: 19237524]
40. Li G, Sanders JM, Bevard MH, Sun Z, Chumley JW, Galkina EV, Ley K, Sarembock IJ. CD40 ligand promotes Mac-1 expression, leukocyte recruitment, and neointima formation after vascular injury. Am J Pathol. 2008; 172:1141–1152. [PubMed: 18349125]
41. Powell JD, Ragheb JA, Kitagawa-Sakakida S, Schwartz RH. Molecular regulation of interleukin-2 expression by CD28 co-stimulation and anergy. Immunol Rev. 1998; 165:287–300. [PubMed: 9850868]
42. Coyle AJ, Gutierrez-Ramos JC. The expanding B7 superfamily: increasing complexity in costimulatory signals regulating T cell function. Nat Immunol. 2001; 2:203–209. [PubMed: 11224518]
43. Vella AT, Mitchell T, Groth B, Linsley PS, Green JM, Thompson CB, Kappler JW, Marrack P. CD28 engagement and proinflammatory cytokines contribute to T cell expansion and long-term survival in vivo. J Immunol. 1997; 158:4714–4720. [PubMed: 9144484]
44. Riley JL, Mao M, Kobayashi S, Biery M, Burchard J, Cavet G, Gregson BP, June CH, Linsley PS. Modulation of TCR-induced transcriptional profiles by ligation of CD28, ICOS, and CTLA-4 receptors. Proc Natl Acad Sci USA. 2002; 99:11790–11795. [PubMed: 12195015]
45. Diehn M, Alizadeh AA, Rando OJ, Liu CL, Stankunas K, Botstein D, Crabtree GR, Brown PO. Genomic expression programs and the integration of the CD28 costimulatory signal in T cell activation. Proc Natl Acad Sci USA. 2002; 99:11796–11801. [PubMed: 12195013]
46. Acuto O, Michel F. CD28-mediated co-stimulation: a quantitative support for TCR signalling. Nat Rev Immunol. 2003; 3:939–951. [PubMed: 14647476]
47. Kappler JW, Herman A, Clements J, Marrack P. Mutations defining functional regions of the superantigen staphylococcal enterotoxin B. J Exp Med. 1992; 175:387–396. [PubMed: 1370682]
48. Remick DG, Bolgos GR, Siddiqui J, Shin J, Nemzek JA. Six at six: interleukin-6 measured 6 h after the initiation of sepsis predicts mortality over 3 days. Shock. 2002; 17:463–467. [PubMed: 12069181]
49. Remick DG, Bolgos G, Copeland S, Siddiqui J. Role of interleukin-6 in mortality from and physiologic response to sepsis. Infect Immun. 2005; 73:2751–2757. [PubMed: 15845478]
50. Damas P, Ledoux D, Nys M, Vrindts Y, De Groote D, Franchimont P, Lamy M. Cytokine serum level during severe sepsis in human IL-6 as a marker of severity. Ann Surg. 1992; 215:356–362. [PubMed: 1558416]

51. Naffaa M, Makhoul BF, Tobia A, Kaplan M, Aronson D, Saliba W, Azzam ZS. Interleukin-6 at discharge predicts all-cause mortality in patients with sepsis. Am J Emerg Med. 2013; 31:1361–1364. [PubMed: 23896015]
52. Cohen J. The immunopathogenesis of sepsis. Nature. 2002; 420:885–891. [PubMed: 12490963]
53. Torres BA, Kominsky S, Perrin GQ, Hobeika AC, Johnson HM. Superantigens: the good, the bad, and the ugly. Exp Biol Med (Maywood). 2001; 226:164–176. [PubMed: 11361034]
54. Huvenne W, Hellings PW, Bachert C. Role of staphylococcal superantigens in airway disease. Int Arch Allergy Immunol. 2013; 161:304–314. [PubMed: 23689556]
55. Wikstrom ME, Stumbles PA. Mouse respiratory tract dendritic cell subsets and the immunological fate of inhaled antigens. Immunol Cell Biol. 2007; 85:182–188. [PubMed: 17262055]
56. Whitsett JA. Intrinsic and innate defenses in the lung: intersection of pathways regulating lung morphogenesis, host defense, and repair. J Clin Invest. 2002; 109:565–569. [PubMed: 11877462]
57. Vermaelen KY, Carro-Muino I, Lambrecht BN, Pauwels RA. Specific migratory dendritic cells rapidly transport antigen from the airways to the thoracic lymph nodes. J Exp Med. 2001; 193:51–60. [PubMed: 11136820]
58. Kaukonen KM, Bailey M, Pilcher D, Cooper DJ, Bellomo R. Systemic inflammatory response syndrome criteria in defining severe sepsis. N Engl J Med. 2015; 372:1629–1638. [PubMed: 25776936]
59. Devi S, Wang Y, Chew WK, Lima R, AGN, Mattar CN, Chong SZ, Schlitzer A, Bakocevic N, Chew S, Keeble JL, Goh CC, Li JL, Evrard M, Malleret B, Larbi A, Renia L, Haniffa M, Tan SM, Chan JK, Balabanian K, Nagasawa T, Bachelerie F, Hidalgo A, Ginhoux F, Kubes P, Ng LG. Neutrophil mobilization via plerixafor-mediated CXCR4 inhibition arises from lung demargination and blockade of neutrophil homing to the bone marrow. J Exp Med. 2013; 210:2321–2336. [PubMed: 24081949]
60. Mourad W, Mehindate K, Schall TJ, McColl SR. Engagement of major histocompatibility complex class II molecules by superantigen induces inflammatory cytokine gene expression in human rheumatoid fibroblast-like synoviocytes. J Exp Med. 1992; 175:613–616. [PubMed: 1732419]
61. Diener K, Tessier P, Fraser J, Kontgen F, McColl SR. Induction of acute inflammation in vivo by staphylococcal superantigens I: Leukocyte recruitment occurs independently of T lymphocytes and major histocompatibility complex Class II molecules. Lab Invest. 1998; 78:647–656. [PubMed: 9645755]
62. Hampton HR, Bailey J, Tomura M, Brink R, Chtanova T. Microbe-dependent lymphatic migration of neutrophils modulates lymphocyte proliferation in lymph nodes. Nat Commun. 2015; 6:7139. [PubMed: 25972253]
63. Bradley JR. TNF-mediated inflammatory disease. J Pathol. 2008; 214:149–160. [PubMed: 18161752]
64. Galea-Lauri J, Darling D, Gan SU, Krivochtchapov L, Kuiper M, Gaken J, Souberbielle B, Farzaneh F. Expression of a variant of CD28 on a subpopulation of human NK cells: implications for B7-mediated stimulation of NK cells. J Immunol. 1999; 163:62–70. [PubMed: 10384100]
65. Venuprasad K, Banerjee PP, Chattopadhyay S, Sharma S, Pal S, Parab PB, Mitra D, Saha B. Human neutrophil-expressed CD28 interacts with macrophage B7 to induce phosphatidylinositol 3-kinase-dependent IFN-gamma secretion and restriction of Leishmania growth. J Immunol. 2002; 169:920–928. [PubMed: 12097397]
66. Pennington JE. Therapy with antibody to tumor necrosis factor in sepsis. Clin Infect Dis. 1993; 17(Suppl 2):S515–519. [PubMed: 8274618]
67. Cohen J, Carlet J. INTERSEPT: an international, multicenter, placebo-controlled trial of monoclonal antibody to human tumor necrosis factor-alpha in patients with sepsis. International Sepsis Trial Study Group. Crit Care Med. 1996; 24:1431–1440. [PubMed: 8797612]
68. Abraham E, Wunderink R, Silverman H, Perl TM, Nasraway S, Levy H, Bone R, Wenzel RP, Balk R, Allred R, et al. Efficacy and safety of monoclonal antibody to human tumor necrosis factor alpha in patients with sepsis syndrome. A randomized, controlled, double-blind, multicenter clinical trial. TNF-alpha MAb Sepsis Study Group. JAMA. 1995; 273:934–941. [PubMed: 7884952]

69. Fisher CJ Jr, Agosti JM, Opal SM, Lowry SF, Balk RA, Sadoff JC, Abraham E, Schein RM, Benjamin E. Treatment of septic shock with the tumor necrosis factor receptor:Fc fusion protein. The Soluble TNF Receptor Sepsis Study Group. N Engl J Med. 1996; 334:1697–1702. [PubMed: 8637514]

70. Bongartz T, Sutton AJ, Sweeting MJ, Buchan I, Matteson EL, Montori V. Anti-TNF antibody therapy in rheumatoid arthritis and the risk of serious infections and malignancies: systematic review and meta-analysis of rare harmful effects in randomized controlled trials. JAMA. 2006; 295:2275–2285. [PubMed: 16705109]

71. von Kockritz-Blickwede M, Rohde M, Oehmcke S, Miller LS, Cheung AL, Herwald H, Foster S, Medina E. Immunological mechanisms underlying the genetic predisposition to severe Staphylococcus aureus infection in the mouse model. Am J Pathol. 2008; 173:1657–1668. [PubMed: 18974303]

72. Bermejo-Martin JF, Tamayo E, Ruiz G, Andaluz-Ojeda D, Herran-Monge R, Muriel-Bombin A, Fe Munoz M, Heredia-Rodriguez M, Citores R, Gomez-Herreras J, Blanco J. Circulating neutrophil counts and mortality in septic shock. Crit Care. 2014; 18:407. [PubMed: 24524810]

73. Suntharalingam G, Perry MR, Ward S, Brett SJ, Castello-Cortes A, Brunner MD, Panoskaltsis N. Cytokine storm in a phase 1 trial of the anti-CD28 monoclonal antibody TGN1412. N Engl J Med. 2006; 355:1018–1028. [PubMed: 16908486]

74. Saha B, Harlan DM, Lee KP, June CH, Abe R. Protection against lethal toxic shock by targeted disruption of the CD28 gene. J Exp Med. 1996; 183:2675–2680. [PubMed: 8676089]

75. Saha B, Jaklic B, Harlan DM, Gray GS, June CH, Abe R. Toxic shock syndrome toxin-1-induced death is prevented by CTLA4Ig. J Immunol. 1996; 157:3869–3875. [PubMed: 8892617]

76. Bone RC. Sir Isaac Newton, sepsis, SIRS, and CARS. Crit Care Med. 1996; 24:1125–1128. [PubMed: 8674323]

77. Tamayo E, Fernandez A, Almansa R, Carrasco E, Heredia M, Lajo C, Goncalves L, Gomez-Herreras JI, de Lejarazu RO, Bermejo-Martin JF. Pro- and anti-inflammatory responses are regulated simultaneously from the first moments of septic shock. Eur Cytokine Netw. 2011; 22:82–87. [PubMed: 21628135]

78. Novotny AR, Reim D, Assfalg V, Altmayr F, Friess HM, Emmanuel K, Holzmann B. Mixed antagonist response and sepsis severity-dependent dysbalance of pro- and anti-inflammatory responses at the onset of postoperative sepsis. Immunobiology. 2012; 217:616–621. [PubMed: 22204813]

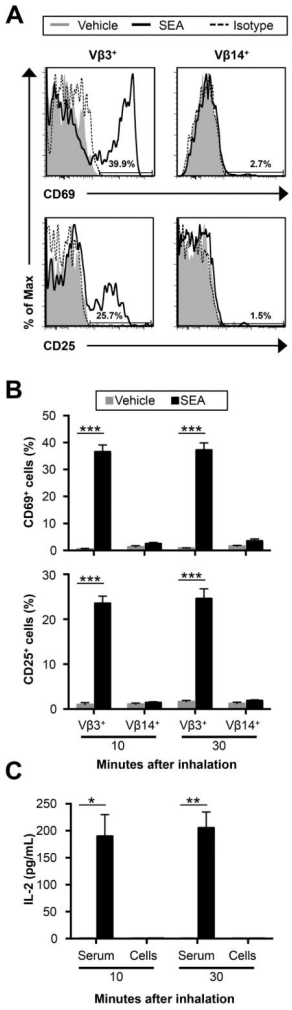

FIGURE 1. After inhalation, SEA circulates systemically via blood

Tail blood was collected 10 or 30 min after SEA or vehicle inhalation and the serum or blood cells were incubated overnight with enriched naïve T cells. The expression of activation markers CD69 and CD25 was measured on SEA-activated $CD3^+V\beta3^+$ T cells and on bystander $CD3^+V\beta14^+$ T cells by flow cytometry. A) Representative histograms of $CD69^+$ and $CD25^+$ cells in $CD3^+V\beta3^+$ and $CD3^+V\beta14^+$ populations after a co-culture of naïve T cells with serum from SEA or vehicle mice. B) Percent of $CD69^+$ and $CD25^+$ cells in $CD3^+V\beta3^+$ and $CD3^+V\beta14^+$ populations after a co-culture of naïve T cells with serum from SEA or vehicle mice. C) Concentration of IL-2 in the supernatants from a co-culture between naïve T cells and serum or cells from blood harvested from SEA or vehicle mice. Data were combined from 3 independent experiments with n=3 in vehicle group and n=6 in SEA group. Data are shown as mean ± SEM. Statistical significance was determined by two-tailed Student's t-tests (*P<0.05; **P<0.01; ***P<0.001).

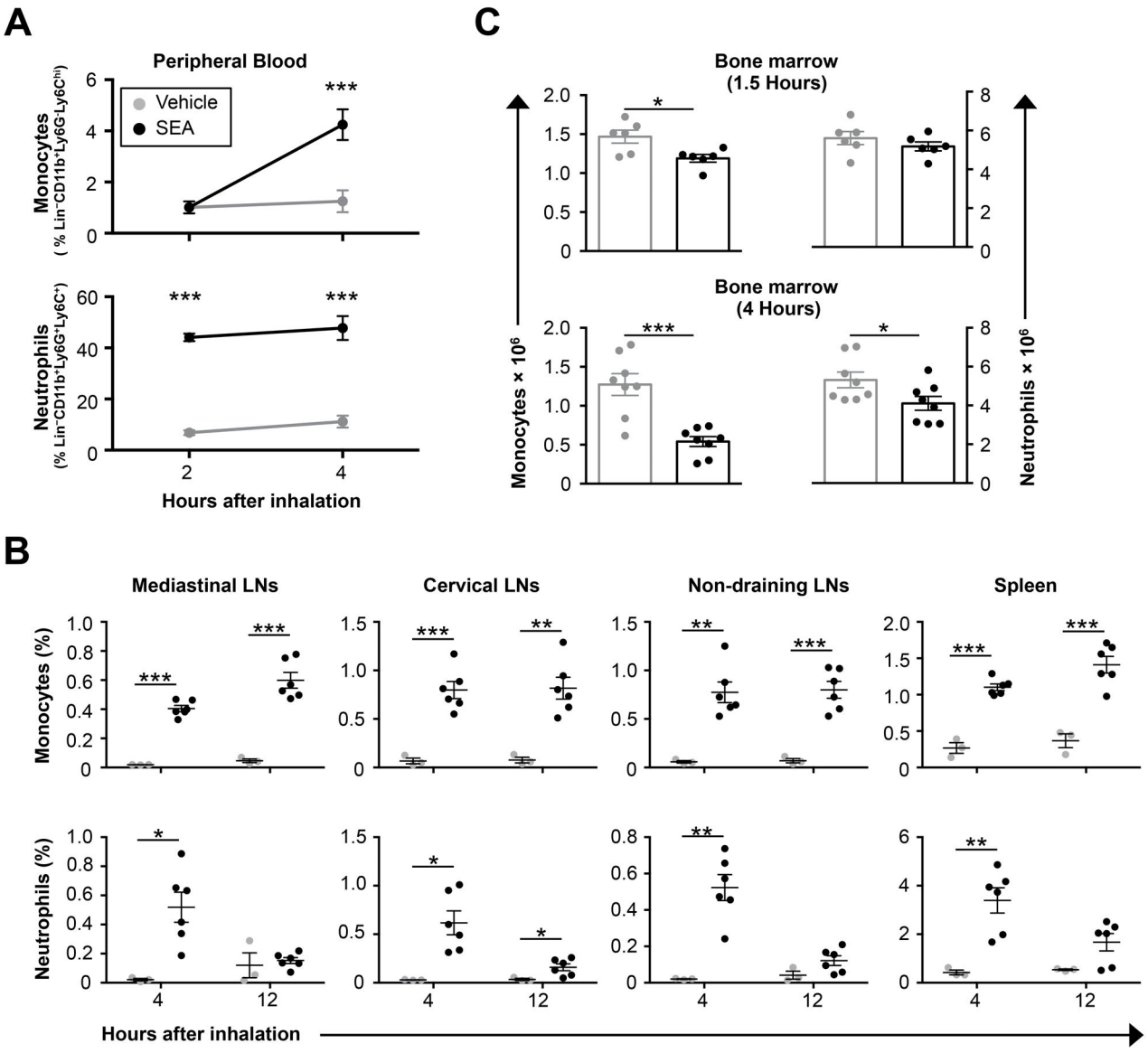

FIGURE 2. SEA inhalation induces systemic migration of inflammatory monocytes and neutrophils

Peripheral blood, BM, LNs and spleen were collected after SEA or vehicle inhalation. The populations of $Lin^{-}(CD3/CD19^{-})CD11b^{+}Ly6G^{-}Ly6C^{hi}$ inflammatory monocytes and $Lin^{-}CD11b^{+}Ly6G^{+}Ly6C^{+}$ neutrophils were detected by flow cytometry. A) Percent of monocytes and neutrophils in peripheral blood 2 and 4 h after SEA or vehicle challenge. Data were combined from 3 independent experiments with n=8 per group. B) Percent of inflammatory monocytes and neutrophils in LNs and spleen 4 and 12 h after SEA or vehicle challenge. Non-draining LNs = axillary, brachial, inguinal, and mesenteric LNs. Data were combined from 3 independent experiments with n=3 for vehicle group and n=6 for SEA group. C) Absolute number of inflammatory monocytes and neutrophils in BM from one femur and tibia 1.5 and 4 h after SEA or vehicle challenge. Data were combined from at least 3 independent experiments with n=6–8 per group. Data are shown as mean ± SEM.

Statistical significance was determined by two-tailed Student's t-tests (*P<0.05; **P<0.01; ***P<0.001).

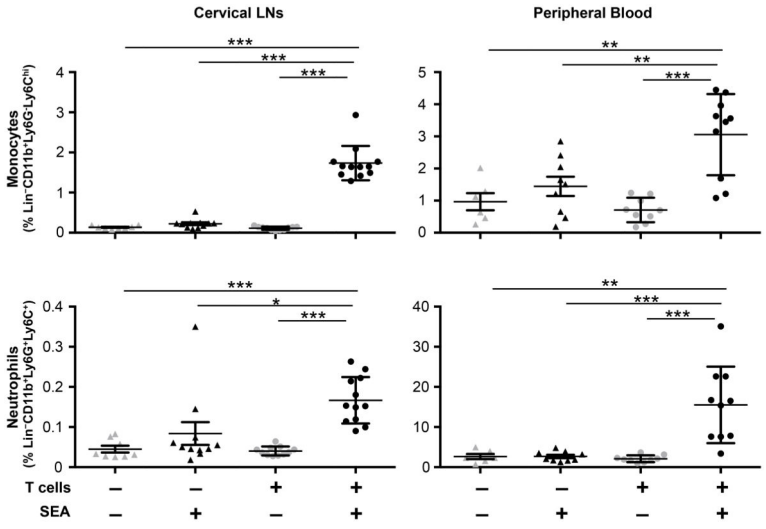

FIGURE 3. T cells are required for the systemic recruitment of inflammatory monocytes and neutrophils after SEA inhalation

TCR $\beta\delta^{-/-}$ mice received C57BL/6J T cells or nothing. On the next day, they were challenged with SEA or vehicle and cervical LNs and peripheral blood were collected 6 h after the challenge to identify $Lin^{-}(CD3/CD19^{-})CD11b^{+}Ly6G^{-}Ly6C^{hi}$ inflammatory monocytes and $Lin^{-}CD11b^{+}Ly6G^{+}Ly6C^{+}$ neutrophils. For cervical LNs, data were combined from at least 4 independent experiments with n = 8–12 per group. For peripheral blood, data were combined from at least 3 independent experiments with n = 6–10 per group. Data are shown as mean ± SEM. Statistical significance was determined by two-tailed Student's t-tests (*P<0.05; **P<0.01; ***P<0.001).

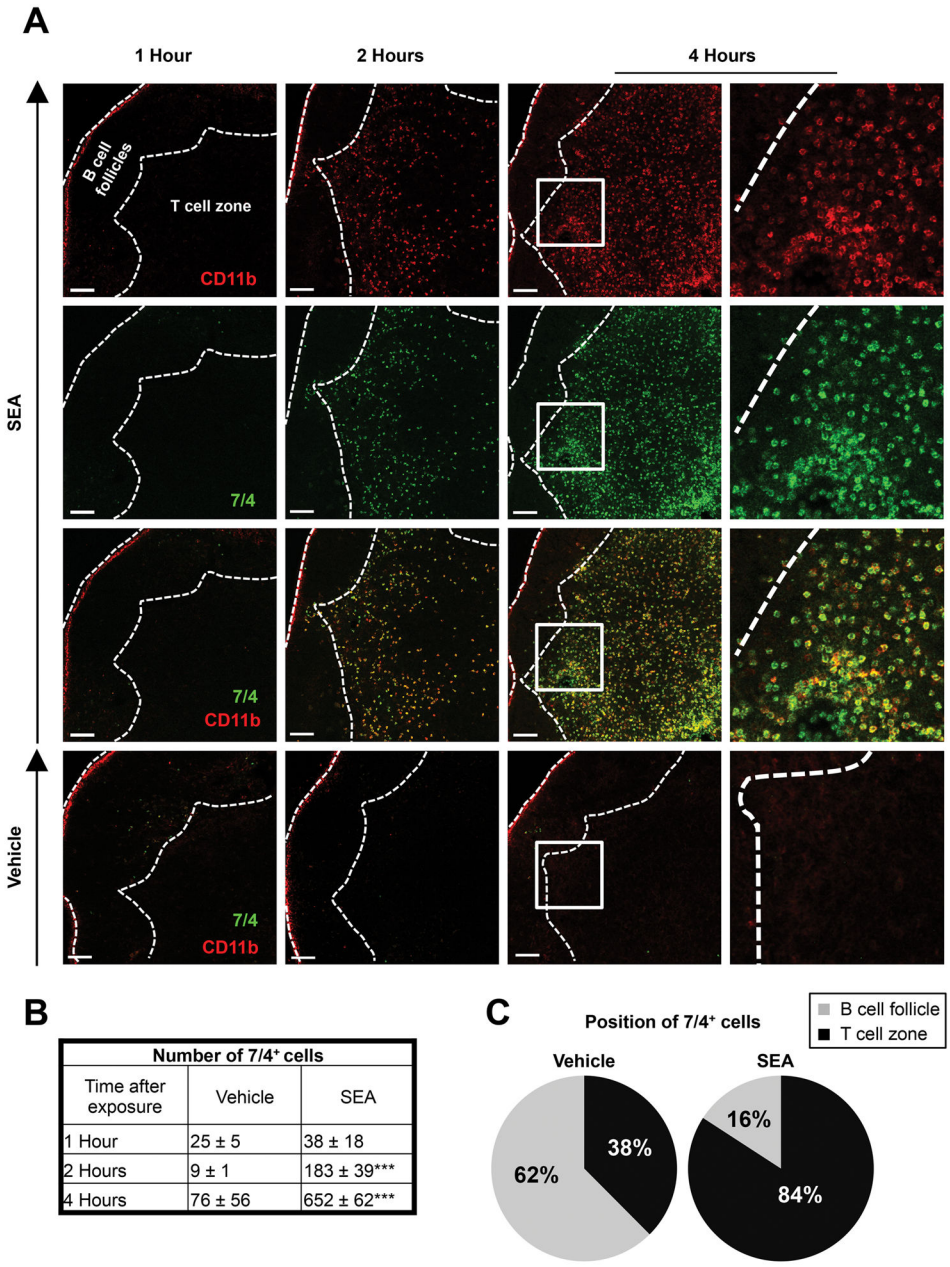

Number of 7/4⁺ cells		
Time after exposure	Vehicle	SEA
1 Hour	25 ± 5	38 ± 18
2 Hours	9 ± 1	183 ± 39***
4 Hours	76 ± 56	652 ± 62***

FIGURE 4. Inflammatory innate immune cells migrate to the T cell zone of the LNs after SEA inhalation

A) Representative confocal microscopy images of frozen sections from cervical LNs 1, 2 and 4 h after SEA or vehicle challenge. Inflammatory innate immune cells (monocytes and neutrophils) were labeled with anti-CD11b and anti-7/4 antibodies. The white dashed line marks B cell follicles and was determined by anti-B220 staining (not shown). The vertical panel on the right represents an enlarged image of the area in the white square. The displayed images are projections of confocal z stacks taken using 20× magnification/0.8 numerical aperture objective and Zeiss LSM780 confocal microscope. Scale bar = 80 μm. B) Number of $7/4^+$ cells. The amount of $7/4^+$ cells per field was determined from 3 images per

mouse by Imaris (Bitplane). Statistical significance was assessed by two-tailed Student's t-tests (***P<0.001). C) Position of 7/4$^+$ cells in LNs. The number of 7/4$^+$ cells in B cell follicles vs. T cell zone was determined from 3 images per mouse by Imaris. The data are representative of least 3 independent experiments with n=3–5 per group.

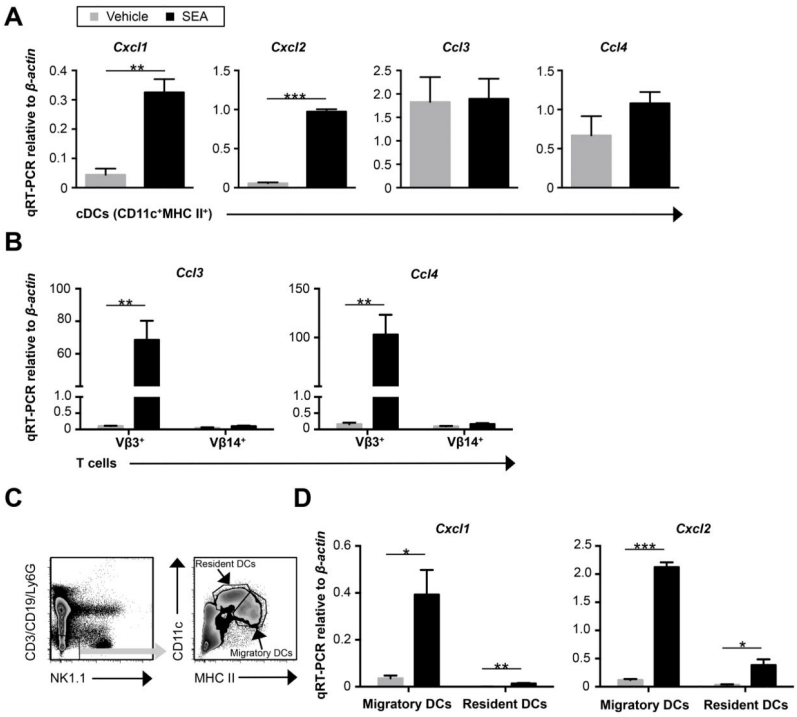

FIGURE 5. T cells and DCs express chemokines after SEA inhalation

LNs (axillary, brachial, inguinal, mesenteric, cervical and mediastinal) were collected 2 h after SEA or vehicle challenge and cells were stained to sort for specific populations. RNA isolated from the sorted populations was used for qRT-PCR analysis. A) Expression of *Cxcl1*, *Cxcl2*, *Ccl3* and *Ccl4* in $CD3^{-}CD19^{-}$ (or $B220^{-}$)$NK1.1^{-}DX5^{-}MHC\ II^{+}CD11c^{+}$ conventional DCs (cDCs). B) Expression of *Ccl3* and *Ccl4* in $V\beta3^{+}$ and $V\beta14^{+}$ T cells. C) Gating strategy to isolate migratory and resident DCs. D) Expression of *Cxcl1* and *Cxcl2* in migratory and resident DCs. Expression of chemokines is shown relative to *β-actin*. Data are displayed as mean + SEM. Data are representative of 3 independent experiments with n=3 per group. Statistical significance was determined by two-tailed Student's t-tests (**P*<0.05; ***P*<0.01; ****P*<0.001).

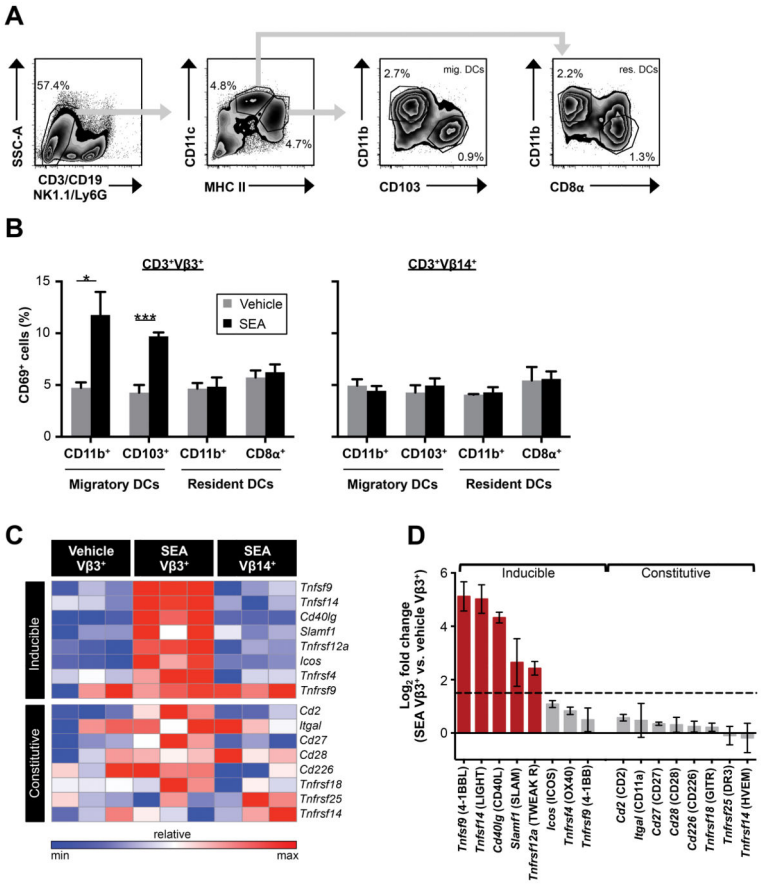

FIGURE 6. Migratory DCs present SEA to T cells leading to expression of inducible costimulatory molecules on T cells

A) Gating strategy used to sort for DC subpopulations. B) CD69 expression on T cells after co-culture with *ex vivo* derived DCs. LNs were harvested 40 min after SEA or vehicle inhalation and the sorted DC subpopulations were co-cultured with naïve T cells. The expression of CD69 was measured on SEA-activated $CD3^+V\beta3^+$ T cells and on bystander $CD3^+V\beta14^+$ T cells by flow cytometry. Data are displayed as mean ± SEM and are representative of 4 independent experiments with n=4 per group. Statistical significance was determined by two-tailed Student's t-tests (*P<0.05; **P<0.01; ***P<0.001). C) Heat map showing expression of inducible and constitutively expressed costimulatory molecules in SEA $V\beta3^+$ T cells and control groups (vehicle $V\beta3^+$ and SEA $V\beta14^+$ T cells) 40 min after SEA or vehicle inhalation. Data are representative of 3 independent experiments with n=3 per group. D) Log_2 fold change in the expression of costimulatory molecules in SEA-activated $V\beta3^+$ T cells compared to vehicle $V\beta3^+$ T cells. Significant difference is represented by a dashed line (≥1.5). Data are displayed as mean ± SEM. Data are representative of 3 independent experiments with n=3 per group.

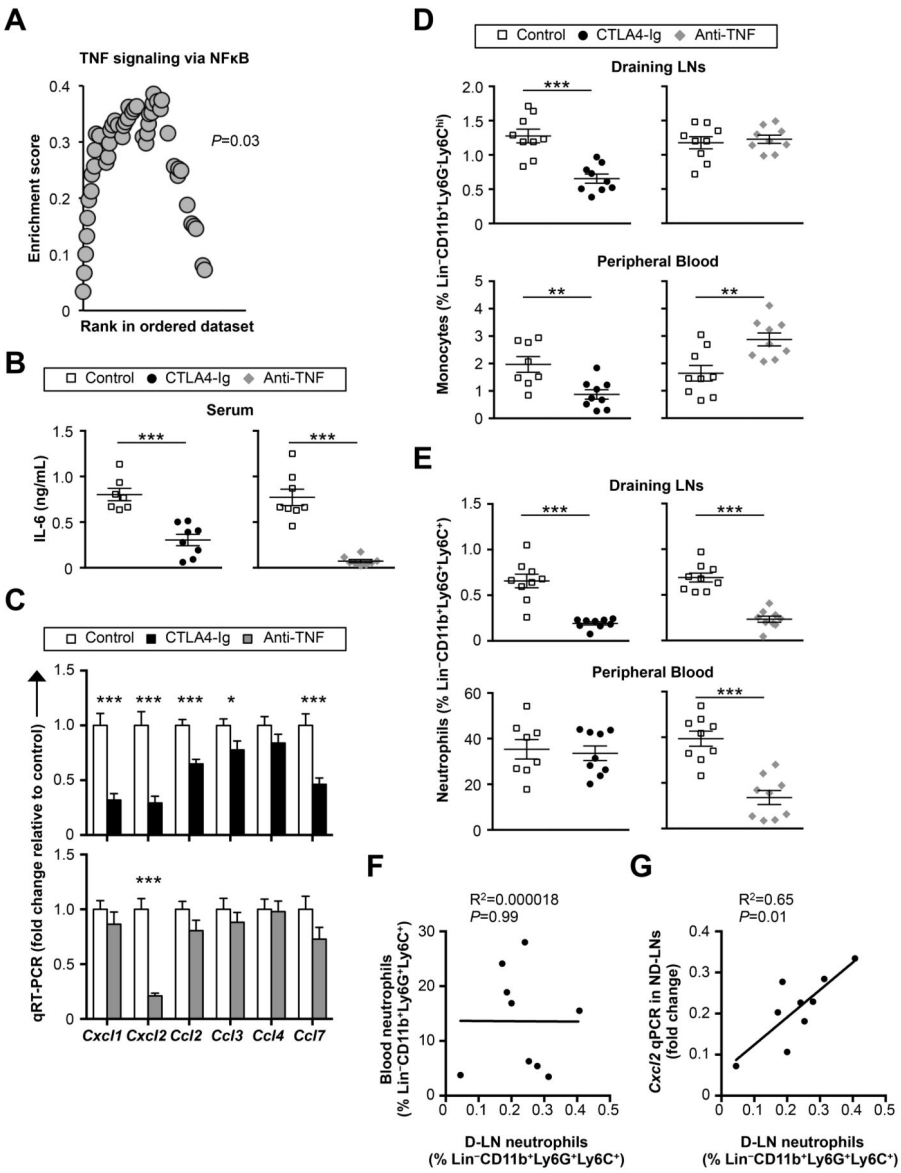

FIGURE 7. The migration of monocytes and neutrophils after SEA inhalation is dependent on CD28 and TNF

A) The NFκB signaling via TNF is upregulated in SEA-activated Vβ3$^+$ T cells 40 min after SEA inhalation. GSEA was used to evaluate significantly enriched pathways in SEA-activated Vβ3$^+$ cells compared to the control groups (vehicle Vβ3$^+$ cells and SEA Vβ14$^+$ cells). Data are representative of 3 independent experiments with n=3 per group. B) Concentration of serum IL-6 in mice treated with CTLA4-Ig or anti-TNF prior to i.n. SEA challenge. Two hours prior to SEA inhalation, mice were treated with CTLA4-Ig or anti-TNF antibody or the respective IgG control i.p. Serum was collected 4 hours after SEA challenge. C) Chemokine expressions in non-draining LNs (mesenteric, axillary, brachial, inguinal) from mice that were treated with either CTLA4-Ig or anti-TNF and the respective IgG control prior pulmonary SEA challenge. Tissue was collected 4 hours after the SEA challenge. The qRT-PCR expression was normalized to *β-actin* and it is expressed as a fold

change relative to the IgG-treated group. D) and E) Percent of Lin^- (CD3/CD19/NK1.1$^-$)$CD11b^+Ly6G^-Ly6C^{hi}$ monocytes (D) and $Lin^-CD11b^+Ly6G^+Ly6C^+$ neutrophils (E) in draining LNs (cervical and mediastinal) and blood in mice treated with CTLA4-Ig or anti-TNF prior to SEA inhalation. Tail blood and draining LNs were collected 4 h after SEA challenge. Data were combined from 3 independent experiments with n=7–9 per group. Data are shown as mean ± SEM. Statistical significance was determined by two-tailed Student's t-tests (*P<0.05; **P<0.01; ***P<0.001). F) and G) Correlating the percent of D-LNs (draining LNs) neutrophils with the percent of neutrophils in blood (F) and ND-LNs (non-draining LNs) *Cxcl2* expression (G). Data are representative of 3 independent experiments with n=9 per group. The P value of the linear regression fit curve is calculated from F test.